

assume that an unknown deep acceptor impurity remains at a constant background value N_x with Zn doping. If capture into this center proceeds via an Auger process whereby a free hole is ejected deep into the valence band, then $1/\tau_n \propto N_x p \propto N_x N_A$.

³⁰T. Miyanchi, H. Sonomura, and N. Yamamoto, *J. Appl. Phys. (Japan)* **8**, 886 (1969).

³¹The temperature dependence of η_{ir}^b for these crystals has been measured [J. M. Dishman (Ref. 2)] and appears very similar to that observed for η_{ir}^a in Fig. 7. The thermal quenching of η_{ir}^b is best explained by taking the lower value $\eta_{ir}^b = 0.13$ in Tables II and III.

³²W. G. Spitzer, M. Gershenson, C. J. Frosch, and D. F. Gibbs, *J. Phys. Chem. Solids* **11**, 339 (1959).

³³L. M. Foster and J. Scardefield, *J. Electrochem. Soc.* **116**, 494 (1969).

³⁴P. J. Dean and C. H. Henry, *Phys. Rev.* **176**, 928

(1968).

³⁵M. Lax, *Phys. Rev.* **119**, 1502 (1960).

³⁶C. K. Kim [*Radiochem. Radioannal. Letters* **2**, 53 (1969)] has found *total* oxygen concentrations of 2×10^{19} cm⁻³ in O-doped solution-grown crystals of GaP comparable to those studied here. M. Kowalchik (unpublished) has found Ga₂O₃ precipitates in GaP(Zn,O) layers grown by liquid-phase epitaxy. Both results suggest the probability of large concentrations of nonsubstitutional O in these samples.

³⁷M. Gershenson, R. A. Logan, and D. F. Nelson, *Phys. Rev.* **149**, 580 (1966).

³⁸H. B. DeVore, *Phys. Rev.* **102**, 86 (1956).

³⁹M. Gershenson and R. M. Mikulyak, *Appl. Phys. Letters* **8**, 245 (1966).

⁴⁰W. Bond (unpublished).

Magnetoresistance and Hall Effect of Hot Electrons in Germanium and Carrier Transfer to Higher Minima*

H. Heinrich and K. Lischka

*Institut für Angewandte Physik der Universität, A-1090 Vienna, Austria
and Ludwig Boltzmann Institut für Festkörperphysik, Vienna, Austria*

and

M. Kriechbaum†

Institut für Theoretische Physik der Universität, A-8010 Graz, Austria

(Received 15 January 1970)

Measurements are reported of the Hall coefficient and the ratio of longitudinal over transverse magnetoresistance in *n*-type Ge up to electric field strengths of 3 and 9 kV/cm, respectively, for $\vec{j} \parallel [100]$ at 200°K, in order to obtain quantitative information about electron transfer to higher conduction-band minima. The lattice temperature was high enough to ensure that no negative differential conductivity was present. Calculations of the galvanomagnetic properties have been performed for the case that (i) electrons are only in the normally occupied $\langle 111 \rangle$ valleys, taking into account acoustical, optical, and equivalent intervalley scattering as well as scattering by ionized impurities; and (ii) electrons are transferred to the higher $\langle 100 \rangle$ conduction-band minima. Only in case (ii) is reasonable agreement between theoretical and experimental results obtained, giving a mobility ratio of only about 4. This is of the same order of magnitude as the theoretical value by Paige.

I. INTRODUCTION

As is well known, the conduction band of germanium consists of four normally occupied minima along the $\langle 111 \rangle$ directions in *k* space, another minimum at the center of the Brillouin zone, and a third set of six minima along the $\langle 100 \rangle$ axis approximately 0.18 eV above the lowest minima.^{1,2} In the past, these higher minima have been considered in influencing the high-field behavior of *n*-type Ge.³⁻⁵ Recently, they have been made re-

sponsible, by Fawcett and Paige,^{6,7} for giving rise to the bulk negative differential resistance⁸ (NDR) by a mechanism similar to that of the Gunn effect in GaAs and to the associated current oscillations observed by McGroddy and Nathan.⁹ It is, however, not yet established¹⁰ whether the influence of the carrier transfer alone is strong enough to cause the NDR or another effect is responsible for it (e.g., Kawamura and Morishita¹¹ and Gueret¹²).

It is the purpose of this paper to present an experimental indication that population of higher val-

leys does occur at high electric fields. We have investigated (i) the longitudinal and transverse magnetoresistance of samples of n -type Ge oriented parallel to the [100] crystallographic direction, at 200 °K up to 9 kV/cm, and (ii) the Hall coefficient up to 3 kV/cm. Hall measurements in GaAs have been reported by Acket¹³ and interpreted already by Omar¹⁴ in terms of carrier transfer to higher minima. Previous measurements of the hot-electron Hall coefficient in Ge by Movchan¹⁵ have been performed at 77 °K. Although these results agree qualitatively with those reported here for 200 °K, the presence of an NDR at 77 °K gives rise to some uncertainty in interpretation of Movchan's data. According to Chang and Ruch,¹⁶ temperatures above 150 °K ensure that the NDR vanishes and, consequently, the interpretation of our measurements is not obscured by the formation of high-field domains. Owing to the fact that the energy relaxation time at high fields and the high-field electron drift mobility show only a slight dependence on lattice temperature, it is to be expected that also at temperatures higher than 150 °K considerable carrier transfer to the higher valleys is present. This will be shown by comparison of the calculations with the experiments. We have also calculated the magnetoresistance of hot electrons with carriers only in the $\langle 111 \rangle$ valleys by taking into account scattering by optical, acoustical, and equivalent intervalley phonons as well as ionized impurities. We will show that the experiments at high electric fields cannot be explained by this simple model and that population of higher minima has to be considered at field strength above 2 kV/cm.

The change in symmetry, when electrons are transferred from the $\langle 111 \rangle$ "germaniumlike" valleys to the $\langle 100 \rangle$ "siliconlike" valleys manifests itself in a strong change in magnetoresistance behavior. Although no theoretical treatment appears to be available at present of hot-electron magnetoresistance, taking into account the band structure of Ge, including the higher valleys, at least a semiquantitative interpretation of the experimental results in terms of a two-band model is possible, as will be shown in Sec. VI.

Similar calculations have been performed for the Hall effect and it was found that also in this case the experimental data could only be understood by means of a two-band conduction mechanism.

To estimate the influence of electron transfer we will calculate the fraction of electrons in the lower and upper valleys by assuming a model with parabolic energy minima and Maxwellian energy distribution and using the energy-balance equation. Similar calculations have been performed for GaAs and GaSb by Omar.^{14,17}

II. EXPERIMENTAL

Filamentary samples were prepared from n -type Ge with 5 Ω cm resistivity at room temperature, with their axis parallel to the [100] crystallographic direction. The samples for the magnetoresistance measurements had a cross section of 0.15 mm² and a length of about 3 mm. The Hall measurements were performed with samples (5 \times 1.7 \times 0.5 mm³) with narrow side arms of 0.2 mm width. Contacts have been prepared by As diffusion and Ni plating of the end faces.

The measuring arrangement is shown in Fig. 1. Fast-rising pulses were applied to the sample by discharging a coaxial cable. The sample has been mounted in an insertion unit inside a Dewar within the magnetic field, and could be rotated from longitudinal to transverse magnetic field positions. The applied voltage and the voltage drop on a small current measuring resistor were observed on an sampling oscilloscope and an X-Y recorder connected to it. In case of magnetoresistance measurements the change of the current due to the application of a magnetic field at constant voltage conditions has been observed. The smallest detectable change of the current was below 10⁻³, by making use of the dc offset of the sampling oscilloscope (Tektronix 661). Hall measurements have been performed by observing the difference signal

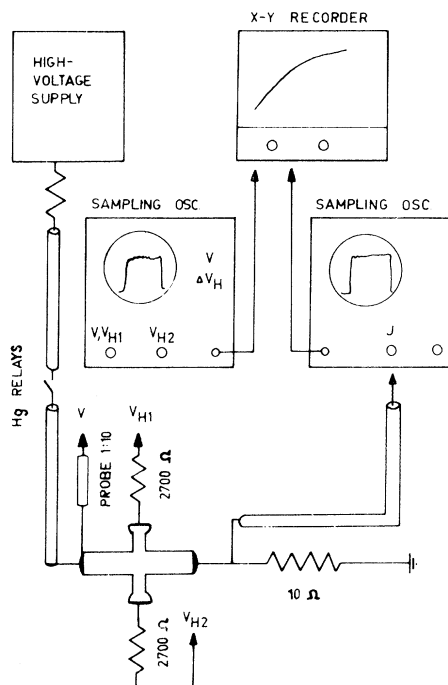


FIG. 1. Schematic diagram of the measuring apparatus.

between the side-arm potentials on a second sampling oscilloscope. The measurements have been taken within 1–3 nsec after application of the pulse to avoid any effects of injections of minority carriers from the anode.

III. ANALYTICAL TREATMENT OF GALVANOMAGNETIC EFFECTS OF HOT ELECTRONS IN (111) VALLEYS

Several authors have treated the problem of hot-electron magnetoresistance in semiconductors. A compilation of previous papers will be found in Ref. 18. Since the galvanomagnetic properties are very sensitive to scattering mechanisms it is felt that only calculations including all possible scattering mechanisms are adequate for comparison with experimental results. We have, therefore, performed a calculation according to a model used in two previous publications,^{19,20} hereafter referred to as I and II, whose main features will be shortly outlined here.

In calculating the current as a function of an externally applied field, one has to solve a Boltzmann equation for the carriers. There are two main difficulties for a semiconductor with spheroidal energy surfaces: (i) Taking into account different scattering mechanisms it is not possible to find the exact distribution function; and (ii) even if one knows the analytic form of the collision operator in the Boltzmann equation exactly, it is not possible to use this exact form in numerical calculations. The second difficulty may be overcome by introducing the concept of relaxation times. This treatment is exact for elastic scattering and randomizing scattering as discussed by Herring and Vogt.²¹ But the acoustic scattering is not elastic, and the optic scattering is not randomizing. But as the energy loss of an electron in a scattering process with an acoustic phonon is small, one may hope that the error by introducing a relaxation time for acoustic scattering is small. The error by introducing a relaxation time for optic scattering may not be too large if the relaxation time for optical scattering is greater than that for acoustic scattering. There are further complications in case of scattering types which are very anisotropic, like ionized impurity scattering as discussed by Eagles and Edwards²² and by Korenblit and Korenblum *et al.*²³ Electron-electron scattering cannot be handled in this way.

To overcome the difficulty regarding the distribution function, approximations are made which depend on the donor concentration under consideration. As has been shown by Fröhlich and Paranjape²⁴ and more exactly by Dykman and Tomchuk,²⁵ there is a limit for the minimum carrier concentration for establishing a Maxwellian energy dis-

tribution with an electron temperature different from the lattice temperature.

In the calculations of this chapter we assume a Maxwell-Boltzmann distribution for the spherical part of the distribution function and consider acoustic, optical, and ionized impurity scattering and intervalley scattering between equivalent valleys. We will use relaxation times for these processes and use the transport theory derived by Herring and Vogt.²¹ We do not take into account the influence of electron-electron scattering on the mobility. So we are able to calculate the Hall-mobility, and magnetoresistance coefficients as a function of the electron temperature. The integration over the energy in calculating the averages of the relaxation time was done numerically. Then we calculated the average energy loss of an electron and with the method of energy balance we calculate the electric field strength necessary to produce the considered electron temperature. The validity of these assumptions will be discussed later on.

The expressions for the relaxation times of the different scattering mechanisms mentioned above and for the energy loss were compiled in I and II. We used also the same constants as listed in II.

In Table I numerical results for the magnetoresistance coefficients are given for the Ohmic case at 300 °K. Since there appears to be some uncertainty in the choice of the correct value of the optical-phonon coupling constant D_{op} , calculated results for three different values of D_{op} are given. However, a variation of D_{op} by a factor of 2 causes only a 5% variation of the calculated magnetoresistance coefficients. Good agreement is obtained with the experimental results of Benedek, Paul, and Brooks²⁶ favoring the lowest value of $D_{op} = 6.4 \times 10^{-4}$ erg/cm given by de Veer and Meyer,²⁷ which we will use in the following.

In order to test the validity of the assumptions, in Fig. 2 the calculated drift velocity is plotted as a function of field strength at 200 °K for current in the [100] direction. From this we calculated the

TABLE I. Comparison of calculated magnetoresistance coefficients ξ_l and ξ_t for different values of the optical-phonon coupling constant D_{op} , and experimental results (Ref. 26) at 300 °K.

	D_{op}	Calculated results			Experimental results
	(erg/cm)	6.4×10^{-4}	9.6×10^{-4}	1.28×10^{-3}	(Ref. 26)
ξ_l		1.087	1.103	1.120	1.09
ξ_t		0.475	0.488	0.502	0.475

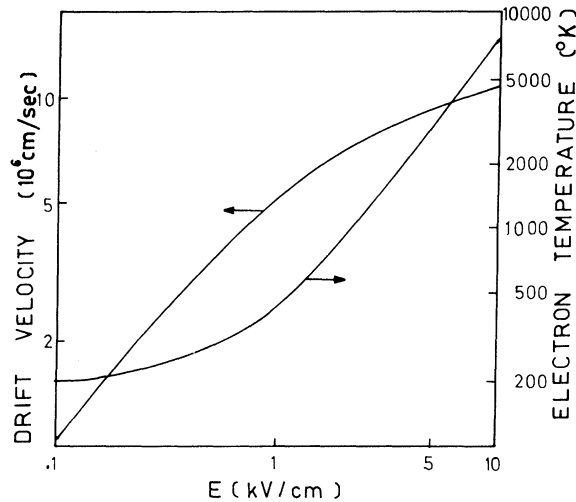


FIG. 2. Calculated values for the drift velocity and electron temperatures assuming that electrons are only in the $\langle 111 \rangle$ valley. Lattice temperature is $T_L = 200^\circ\text{K}$, and $\mathbf{j} \parallel [100]$.

mean relaxation time and from the calculated electron temperature which is also given in Fig. 2, the minimum carrier concentration is obtained at which a Maxwellian distribution is realized according to Fröhlich and Paranjape.²⁴ This criterion is fulfilled only up to a field strength of 0.4 kV/cm at 200°K for a carrier concentration of $3 \cdot 10^{14} \text{ cm}^{-3}$ as used in the present experiments. In calculating the acoustic relaxation time the Planck distribution was used for the phonons. For a high ratio of electron temperature to lattice temperature this may cause a considerable error. But as shown by Meyer and Jørgensen²⁸ we are far away from this critical ratio. The mean optical relaxation time is greater by a factor 10 than the mean acoustic relaxation time up to electron temperatures of 7000°K which corresponds to 10 kV/cm for $T_L = 200^\circ$. Therefore, we may hope that our calculations are close to reality. Especially the ratio of longitudinal to transverse magnetoresistance may be correct because both magnetoresistance coefficients are compiled by similar linear combinations of energy averages of components of the relaxation time tensor. The coefficients of the linear combinations depend only on the particular arrangement of the valleys in k space, as given by Herring and Vogt.²¹ [See Table I and Eqs. (21) and (22) of that paper.] So we expect that the errors introduced by averaging over an incorrect distribution function may partly cancel in calculating the ratio and that the failure of the Fröhlich-Paranjape criterion would not affect the validity of this ratio at high field strengths.

IV. EXPERIMENTAL RESULTS AND CALCULATED VALUES FOR ELECTRONS IN $\langle 111 \rangle$ VALLEYS

The lattice temperature at which the measurements have been performed was well above the maximum value for negative differential conductivity as given by Chang and Ruch.¹⁶ Consequently, no oscillations have been observed and we may attribute the observed phenomena as due to the bulk properties of the material.

Measurements of the magnetoresistance ratio $\Delta\rho_l/\Delta\rho_t$, where $\Delta\rho$ is the change in resistivity due to the application of the magnetic field, have been performed at 200°K for both longitudinal and transverse magnetic fields. For a given value of the electric field, measurements have been made for several values of the magnetic field B , with the product $\mu(E)B$ in the order of 0.1, $\mu(E)$ being the electric-field-dependent electron mobility and B being the magnetic induction. The ratio $\Delta\rho/\rho B^2$ was plotted versus B and extrapolated for B approaching 0.

In Fig. 3 results are given for a typical sample. We plot the ratio of the longitudinal over the transverse magnetoresistance $\Delta\rho_l/\Delta\rho_t|_{B \rightarrow 0}$ as a function of the electric field strength. In this way the strong dependence of the magnetoresistance on $\mu(E)$ is eliminated. Also given are calculated results assuming electrons only in the $\langle 111 \rangle$ valleys. The calculation gives the correct Ohmic value, and both the experimental and theoretical values of $\Delta\rho_l/\Delta\rho_t$ decrease with increasing field. Up to

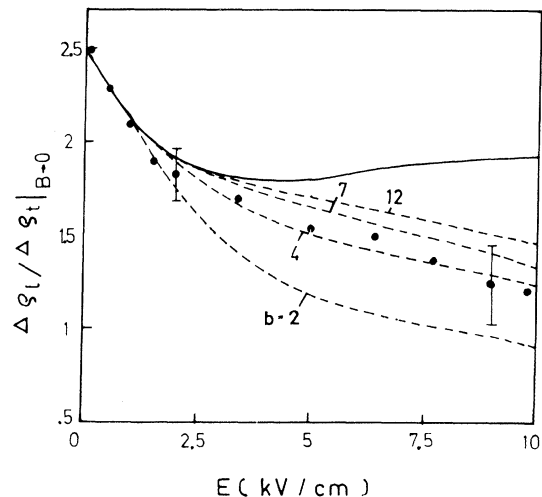


FIG. 3. Ratio of longitudinal over transverse magnetoresistance for the limit of vanishing B . Dots are experimental values at $T_L = 200^\circ\text{K}$ and $\mathbf{j} \parallel [100]$. The full line is calculated for electrons only in $\langle 111 \rangle$ valleys. Dashed lines are calculated for several values of the mobility ratio b with inclusion of electron transfer to $\langle 100 \rangle$ valleys and nonequivalent intervalley scattering.

about 2 kV/cm reasonable agreement is obtained between calculated and experimental results. However, for higher field strength an increasing discrepancy is observed. We, therefore, may conclude, that the described model is not applicable for field strength larger than about 2 kV/cm.

The normalized Hall coefficient (R_H/R_{H0}) is plotted in Fig. 4 as a function of applied electric field. The experimental values exhibit qualitatively the same behavior as the results reported by Movchan and Miselyuk¹⁴ at 77 °K, that is, R_H/R_{H0} shows a strong increase with increasing electric field. In our case, however, the effect is not as pronounced as reported by Movchan and Miselyuk. This may be caused by the difference in lattice temperature or by a inhomogenous field distribution at 77 °K due to the presence of a NDR. The measurements of Fig. 4 have been performed at two different magnetic fields which give about the same results. Therefore, we can rule out the possibility that the observed behavior is caused by a variation of the scattering coefficient ν in the Hall constant due to a change in the value $\mu(E)B$ with increasing electric fields and decreasing $\mu(E)$. Also given in Fig. 4 are calculated results for electrons in $\langle 111 \rangle$ valleys. Although the theoretical results show a small increase in R_H/R_{H0} in the range 0.5–1.5 kV/

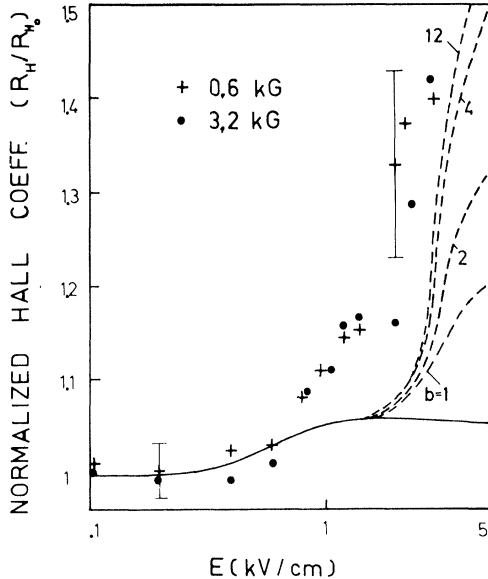


FIG. 4. Normalized Hall coefficient R_H/R_{H0} as a function of electric field at $T_L=200$ °K and $\vec{j} \parallel [100]$. Experimental points are obtained at two different magnetic field values. The full line is calculated for electrons only in $\langle 111 \rangle$ valleys. Dashed lines are calculated for several values of the mobility ratio b with inclusion of electron transfer to $\langle 100 \rangle$ valleys and nonequivalent intervalley scattering.

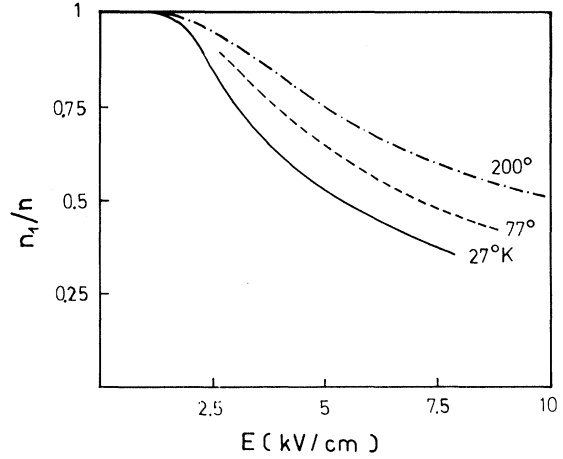


FIG. 5. Calculated values of the ratio n_1/n of carrier densities in the $\langle 111 \rangle$ valleys over total density with $\vec{j} \parallel [100]$. Full and dashed curves: results obtained by Paige⁷ for 27 and 77 °K,³⁰ respectively. Dash-dotted line: present calculations for 200 °K.

cm, they cannot explain the strong rise in the experimentally determined Hall coefficient at strong electric fields. As in the case of the magnetoresistance we conclude that the model used for the calculations is not appropriate for strong electric fields in Ge.

V. ELECTRON TRANSFER TO HIGHER CONDUCTION-BAND MINIMA

Both the behavior of magnetoresistance and the Hall effect may be understood qualitatively if we assume carrier transfer to the $\langle 100 \rangle$ minima and take into account two-band conduction in $\langle 111 \rangle$ and $\langle 100 \rangle$ valleys. In case of the magnetoresistance, carriers in the $\langle 100 \rangle$ valleys do not contribute to the longitudinal magnetoresistance and, therefore, the ratio of longitudinal over transverse magnetoresistance should decrease with increasing carrier transfer. At these conditions one expects that the Hall coefficient increases and should exhibit a maximum at high transfer values.

In order to get quantitative results one needs to know the amount of carrier transfer to the $\langle 100 \rangle$ conduction-band minima. In the following we will neglect the contribution of the $[000]$ valley to the transport properties because of its small effective density of states.⁷ Calculations for lattice temperatures of 27 and 77 °K have been performed by Fawcett and Paige⁶ and Paige,^{7,29} based on a Monte Carlo method. These results are given in Fig. 5. For comparison with the experimental results at 200 °K our calculations have been performed using a model introduced by Omar.¹⁷ From the experimentally determined drift velocity which is an

average over both kinds of valleys ($\langle v_d \rangle$, Fig. 6) the electron temperature has been calculated from the equation

$$e\langle v_d \rangle E = (\epsilon\{T_e\} - \epsilon\{T_L\})/\tau_\epsilon. \quad (1)$$

Here E is the electric field strength, $\epsilon\{T\}$ is the average energy of the electrons calculated according to Omar,¹⁷ and T_e and T_L are electron and lattice temperature, respectively. A value of $\tau_\epsilon = 5 \times 10^{-12}$ sec has been used for the energy relaxation time which has been obtained from the paper by Seeger and Schweizer,³⁰ and which has been found to be fairly constant at high electric fields. Having determined T_e , the numbers n_1 and n_2 of electrons in $\langle 111 \rangle$ and $\langle 100 \rangle$ valleys can be calculated according to Ref. 17 and the results are shown in Fig. 5 for n_1/n . The same constants have been used as quoted in Ref. 7, Table I, from which a value of the effective density-of-states ratio $\alpha = 2.5$ is obtained. α is the effective density of states in all $\langle 100 \rangle$ valleys relative to those in all $\langle 111 \rangle$ valleys.

Despite our very crude model, our data at 200 °K show the general behavior exhibited by the Monte Carlo calculation at 27 and 77 °K,²⁹ except that in our case a more gradual electron transfer at low electric fields is obtained. This good agreement is certainly caused by the fact that the calculations are based on the experimental drift velocity and, therefore, the electron temperature calculated from Eq. (1) will not be in error too much.

VI. TWO-BAND CONDUCTION

Having determined the population ratios in both types of valleys as a function of the applied elec-

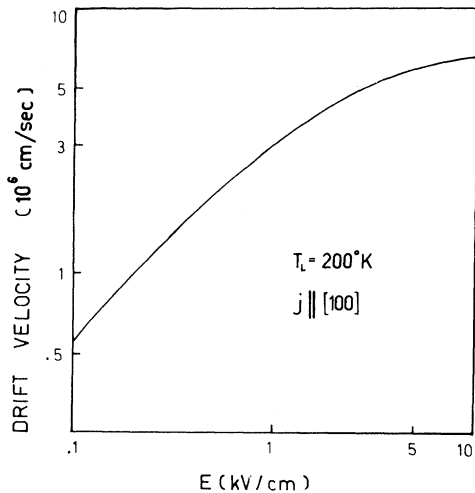


FIG. 6. Experimental drift velocity at $T_L = 200^\circ\text{K}$ and $\vec{j} \parallel [100]$.

tric field, the galvanomagnetic effects can be calculated. In the following we will neglect that for current in $[100]$ direction the $\langle 100 \rangle$ minima are not equivalent and that electrons will accumulate in the cooler $[100]$ valley.

In addition to the scattering mechanisms described in Sec. III we have now to consider the scattering process of electrons from the $\langle 111 \rangle$ valleys into the $\langle 100 \rangle$ valleys as a further scattering mechanism. This case has been treated by Nathan, Paul, and Brooks³¹ by introducing

$$\frac{1}{\tau_{1-2}} = A \frac{(\epsilon - \Delta)^{1/2}}{\epsilon^{1/2}} \frac{1}{\tau_1}, \quad (2)$$

where τ_{1-2} is the relaxation time for scattering from a $\langle 111 \rangle$ into a $\langle 100 \rangle$ valley, and τ_1 the relaxation time for all scattering mechanisms in the $\langle 111 \rangle$ valley. Δ is the energy separation between $\langle 111 \rangle$ and $\langle 100 \rangle$ valleys, ϵ is the carrier energy above the bottom of the $\langle 111 \rangle$ valleys. A was found to be equal to 1 from measurements of the mobility dependence on hydrostatic pressure. The relaxation-time tensor is now

$$\frac{1}{\tau_\perp} = \frac{1}{\tau_{\perp,1}} + \frac{1}{\tau_{1-2}}, \quad \frac{1}{\tau_{\parallel}} = \frac{1}{\tau_{\parallel,1}} + \frac{1}{\tau_{1-2}}, \quad (3)$$

where $\tau_{\perp,1}$ and $\tau_{\parallel,1}$ are the transverse and longitudinal components which were used for the calculations of Sec. III. As the mobility without magnetic field is mainly determined by τ_\perp , we calculated τ_{1-2} by inserting $\tau_{\perp,1}$ for τ_\perp in Eq. (2). The galvanomagnetic effects in the $\langle 111 \rangle$ valleys have been calculated with the relaxation-time tensor Eq. (3) in the limit of zero magnetic field.

The average total drift mobility is then given by

$$\langle \mu \rangle = \mu_1 n_1/n + \mu_2 n_2/n,$$

or by introducing $b = \mu_1/\mu_2$,

$$\langle \mu \rangle = [1 + n_1/n(b-1)]\mu_1/b. \quad (4)$$

Subscripts 1 and 2 refer to $\langle 111 \rangle$ and $\langle 100 \rangle$ valleys, respectively.

The Hall coefficient is given by³²

$$R = -\frac{n}{e} \frac{r_1 b^2 n_1/n + r_2 n_2/n}{(b n_1/n + n_2/n)^2}, \quad (5)$$

where we have assumed that the ratios of the Hall mobilities in $\langle 111 \rangle$ and $\langle 100 \rangle$ are equal to the ratios of the drift mobilities. The scattering coefficient r_2 is assumed to be equal to 1. With the same assumptions the ratio of longitudinal over transverse magnetoresistance is given by³²

$$\frac{\Delta \rho_l}{\Delta \rho_t} = \frac{(n_1/n_2) b^3 \xi_{1l} (1 + b n_1/n_2)}{(n_1/n_2) b (b+1)^2 + [(n_1/n_2) b^3 \xi_{1l} + \xi_{2l}] (1 + b n_1/n_2)}, \quad (6)$$

where ξ_{1l} , ξ_{1t} , and ξ_{2t} are the longitudinal and transverse magnetoresistance coefficients.

Calculated results for $\Delta\rho_l/\Delta\rho_t$ and R_H/R_{H0} according to Eqs. (5) and (6) are given in Figs. 3 and 4, where b has been treated as an adjustable parameter. From analogy to Si,³³ the longitudinal magnetoresistance coefficient ξ_{2t} should be very small and has been taken as equal to zero. In absence of a better value for ξ_{2t} we will use the one reported³³ for Si: $\xi_{2t} = 0.65$.

VII. DISCUSSION

From Figs. 3 and 4 it is clear that much better agreement is obtained between theoretical and calculated values when electron transfer to the $\langle 100 \rangle$ valleys is taken into account. The experimental values of the magnetoresistance fall within the range of the calculated results, indicating a mobility ratio of about 4 over a wide range of electric field strength. However, at strong fields the measuring accuracy becomes comparatively poor and the value of 4 may be taken as indicative only. This may be compared to $b = 2.3$, calculated by Paige for 27 °K and which has been found to be nearly field independent between 2.5 and 7.5 kV/cm.

In the case of the Hall effect the quantitative agreement is less satisfying. Although the calculated results do show the strong increase in R_H/R_{H0} , it occurs at somewhat higher electric field values. The slope of the experimental curve at strong field is best represented by the calculated values with b in the range of 4. The discrepancy between calculated and experimental results of R_H/R_{H0} at intermediate electric field strength has also been observed¹⁶ in GaAs, where it was found that with increasing field intensity the experimental ratio R_H/R_{H0} increases stronger than the calculated one.

We conclude that the experimental values of the galvanomagnetic properties may be understood in terms of the electron-transfer model. Population of the $\langle 100 \rangle$ minima should therefore be taken into account in interpreting high-field effects in n -type Ge. Although the necessity of including the higher valleys has been pointed out several times in the past,^{3-5,34} quantitative calculated results of carrier transfer as a function of the electric field have been published only by Paige⁷ for the case of 27 and 77 °K.³⁰ Our data at 200 °K (Fig. 5) fit into the general scheme of Paige's results, and from the agreement of theoretically and experimentally determined galvanomagnetic properties we may conclude that the values in Fig. 5 are close to reality.

ACKNOWLEDGMENTS

We want to express our appreciation to Professor K. Baumann and Professor K. Seeger for their continuous interest in this work and for many helpful discussions; and to Dr. E. G. S. Paige for providing the data at 77 °K. Thanks are also due the Mathematisches Institut der Technischen Hochschule and the Institut für Statistik der Universität, Vienna, for making available their computer facilities, and to Viki Koeber for preparing the samples.

*Work supported by Fonds zur Förderung der wissenschaftlichen Forschung in Österreich and in part by National Research Council Grant No. A6016, Canada.

¹Present address: Lakehead University, Port Arthur, Canada.

¹M. Cardona and F. H. Pollak, *Phys. Rev.* **142**, 530 (1966).

²A. Jayaraman, B. B. Kosicki, and J. C. Irvin, *Phys. Rev.* **171**, 836 (1968).

³S. H. Koenig, I. N. Marshall, W. Paul, and A. C. Smith, *Phys. Rev.* **118**, 1217 (1960).

⁴H. Risken and H. J. G. Meyer, *Phys. Rev.* **123**, 416 (1961).

⁵E. G. S. Paige, *Progress in Semiconductors* (Heywood, London, 1964), Vol. VIII, p. 200.

⁶W. Fawcett and E. G. S. Paige, *Electron. Letters* **3**, No. 11 (1967).

⁷E. G. S. Paige, *IBM J. Res. Develop.* **13**, 561 (1969).

⁸B. J. Elliott, J. B. Gunn, and J. C. McGroddy, *Appl. Phys. Letters* **11**, 253 (1967).

⁹J. C. McGroddy and M. I. Nathan, *IBM J. Res. Develop.* **11**, 337 (1967).

¹⁰J. E. Smith and J. C. McGroddy, *Appl. Phys. Letters* **11**, 372 (1967).

¹¹M. Kawamura and S. Morishita, *Proc. IEEE* **56**, 1213 (1968).

¹²P. Gueret, *Electron. Letters* **5**, 248 (1969).

¹³G. A. Acket, *Phys. Letters* **25A**, 374 (1967).

¹⁴M. A. Omar, *Phys. Letters* **26A**, 322 (1968).

¹⁵E. A. Movchan and E. G. Miselyuk, *Soviet Phys. Semicond.* **1**, 1047 (1969).

¹⁶D. M. Chang and J. G. Ruch, *Appl. Phys. Letters* **12**, 111 (1968).

¹⁷M. A. Omar, *Phys. Rev.* **171**, 925 (1968).

¹⁸B. R. Nag and H. Paria, *Phys. Rev.* **150**, 632 (1966).

¹⁹H. Heinrich and M. Kriechbaum, *J. Phys. Chem. Solids* **31**, 927 (1970).

²⁰M. Kriechbaum and H. Heinrich, *J. Phys. Chem. Solids* (to be published).

²¹C. Herring and E. Vogt, *Phys. Rev.* **101**, 944 (1956).

²²P. M. Eagles and D. M. Edwards, *Phys. Rev.* **138**, A1706 (1964).

²³I. Ya. Korenblit, *Fiz. Tverd. Tela* **4**, 168 (1962) [*Soviet Phys. Solid State* **4**, 120 (1962)]; I. Ya. Korenblum, A. G. Samoilovich, I. V. Dakhovskii, and V. D.

Iskra, *ibid.* **3**, 2939 (1961) [*ibid.* **3**, 2148 (1962)].

²⁴H. Fröhlich and B. V. Paranjape, Proc. Phys. Soc. (London) **B69**, 21 (1956).

²⁵I. M. Dykman and P. M. Tomchuk, Fiz. Tverd. Tela **2**, 2228 (1960) [Soviet Phys. Solid State **2**, 1988 (1961)].

²⁶G. B. Benedek, W. Paul, and H. Brooks, Phys. Rev. **100**, 1129 (1955).

²⁷S. M. de Veer and H. J. G. Meyer, in *Proceedings of the International Conference on the Physics of Semiconductors, Exeter* (The Institute of Physics and the Physical Society, London, 1962), p. 358.

²⁸N. I. Meyer and M. H. Jørgensen, J. Phys. Chem. Solids **20**, 823 (1965).

²⁹E. G. S. Paige (private communication).

³⁰K. Seeger and D. Schweizer, J. Phys. Soc. Japan Suppl. **21**, 415 (1966).

³¹M. I. Nathan, W. Paul, and H. Brooks, Phys. Rev. **124**, 391 (1961).

³²R. A. Smith, *Semiconductors* (Cambridge U. P., Cambridge, England, 1964).

³³M. Glicksman, Phys. Rev. **105**, 865 (1957).

³⁴E. M. Conwell, Phys. Rev. **135**, A1138 (1964).

Spectroscopic Study of the Deformation-Potential Constants of Group-III Acceptors in Germanium[†]

R. L. Jones* and P. Fisher

Department of Physics, Purdue University, Lafayette, Indiana 47907

(Received 27 February 1970)

The effect of uniaxial compression on the excitation spectra of group-III impurities in germanium is presented and discussed. The deformation-potential constants b' and d' for the ground states are deduced on the basis of the piezospectroscopic effects for the C and D lines. Although there is a slight chemical-species dependence of b' and d' , the average values of these are -1.4 and -2.5 eV, respectively. These, in turn, lead to the values of -2.5 and -4.1 eV for b and d , the corresponding parameters for the valence band, using the relationships given by Bir *et al.* The values of b and d thus calculated agree in sign and magnitude with those determined by other methods. This is in contrast to the results obtained on the basis of the previous interpretation, in which the final state of the B line is assumed to have Γ_7 symmetry.

I. INTRODUCTION

A study of the electronic excitation spectra of impurities in semiconductors under uniaxial strain provides direct information about the deformation-potential constants of the energy states of the impurity. In the case of group-V impurities in germanium or silicon, the stress-induced splittings of the excited p states are the same¹⁻³ as those of the conduction-band minima; hence the corresponding deformation-potential constant of the host can also be readily obtained from the piezospectroscopy of the impurities. For the shallow donors, the dependence of the ground states on the applied force is relatively simple and well understood.¹⁻³ Because of the complexity of the top of the valence bands of silicon and germanium, the effective-mass description of the shallow acceptor impurities⁴⁻⁶ in these materials is considerably more complicated than for the group-V donors.⁴ The effective-mass wave equation for acceptors consists of a set of coupled differential equations, each involving all

valence-band edges. Thus, under the effect of a uniaxial force, the sublevels of an excited impurity state do not follow a given band edge in a simple manner, as is the case for the group-V impurities. In fact, as discussed by Bir *et al.*⁷ and Suzuki *et al.*,⁸ an explicit relationship between the splitting of the ground state of a group-III acceptor and that of the valence-band edge can only be obtained from a detailed knowledge of the wave functions of the impurity state. These authors have used the effective-mass wave functions for this purpose. Given the deformation-potential constants of the impurity state, such an approximation should be sufficient to predict the correct sign of the valence-band deformation-potential constants, if not the magnitude.

The first piezospectroscopic study of a group-III impurity in silicon or germanium was that of Jones and Fisher for thallium in germanium.⁹ More recently, a study was made of group-III impurities in germanium by Dickey and Dimmock¹⁰ and group-III impurities in silicon by Onton *et al.*¹¹ The inter-